

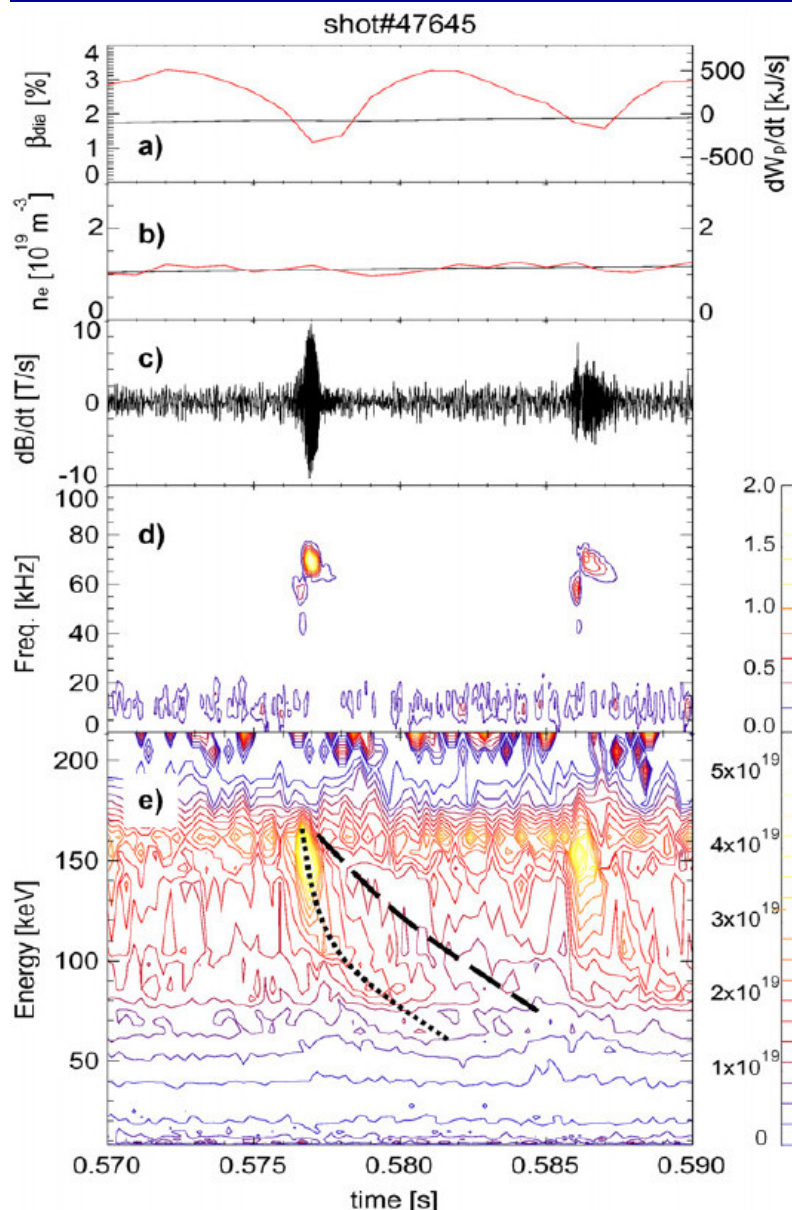
Observation of Hole-Clump Pair Using an Upgraded E//B-NPA during TAE Burst in LHD

S. Kamio, Y. Fujiwara, K. Nagaoka, K. Ogawa, R. Seki, H. Nuga,
M. Isobe, M. Osakabe, and the LHD Experiment Group

National Institute for Fusion Science

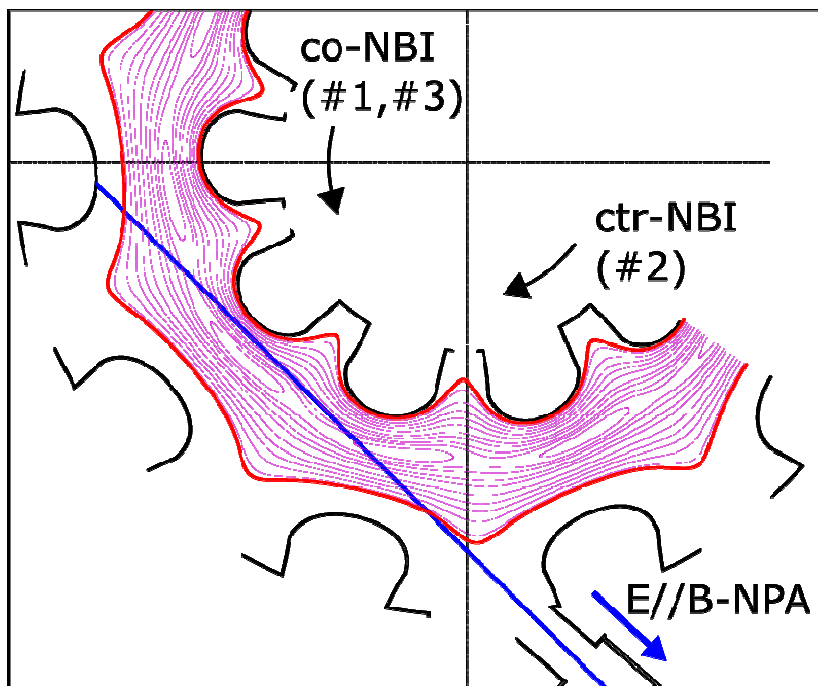


Previous research of TAE burst in LHD

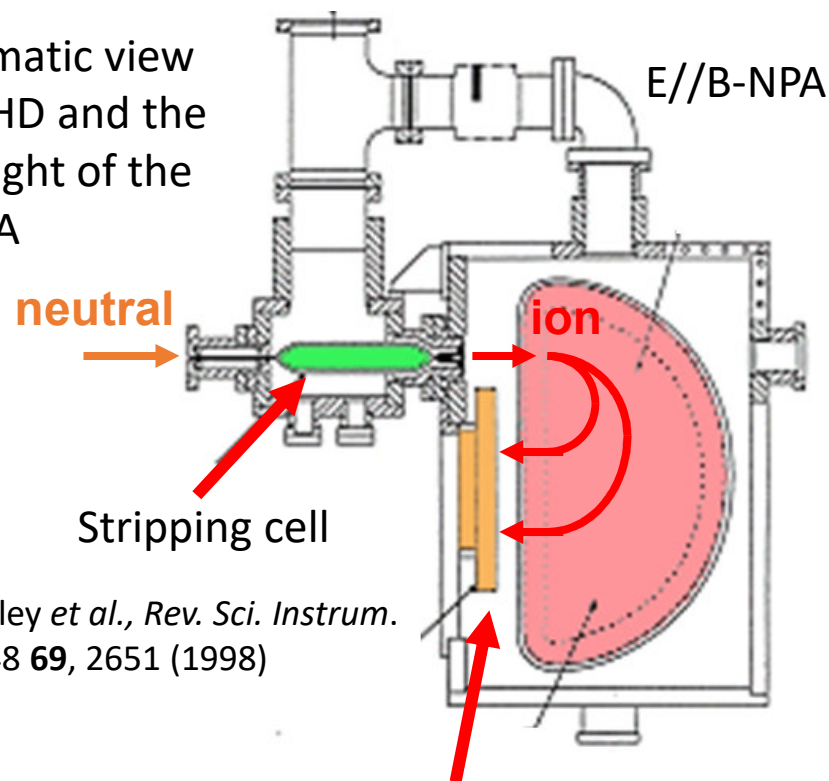


- The toroidal Alfvén eigenmodes (TAE) was investigated in LHD using E//B-NPA.
- The magnetic fluctuations of the TAE bursts are observed in the low magnetic field experiments.
- By the E//B-NPA measurement, clump and hole creations were observed.
- From the slowing down time analysis, the location of each orbit was identified.
- Simultaneous observation of clump and hole formations reveal the enhanced radial transport of energetic particles in plasma by TAE bursts.

E//B-NPA Diagnostic for EP measurement

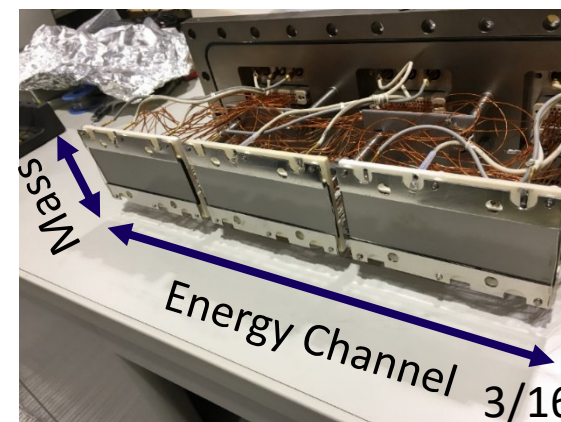


← Schematic view of the LHD and the line of sight of the E//B-NPA

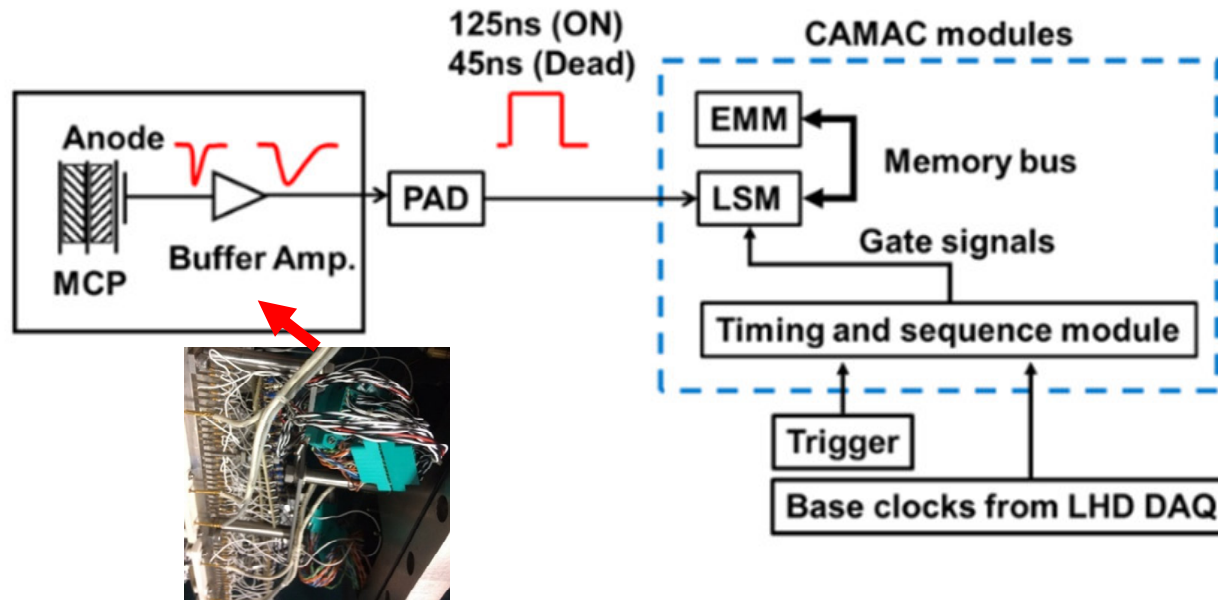


S. S. Medley *et al.*, *Rev. Sci. Instrum.* 0034-6748 **69**, 2651 (1998)

Photographs of the E//B-NPA



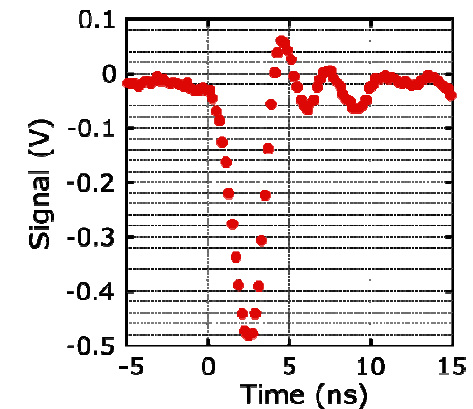
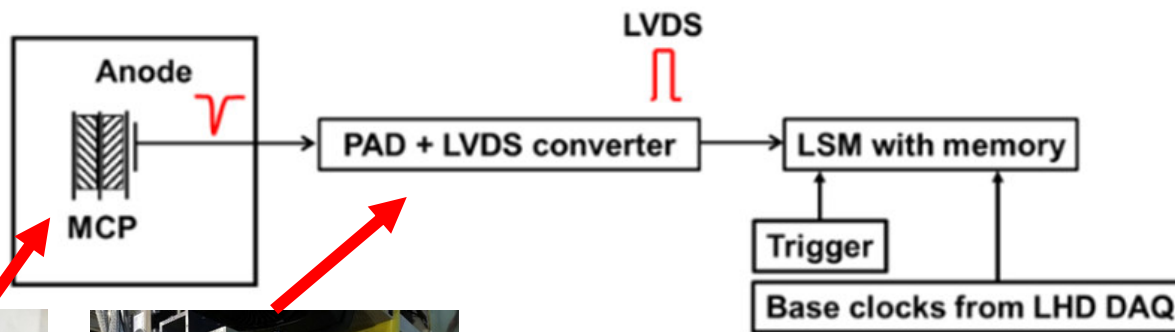
Upgrade of the E//B-NPA



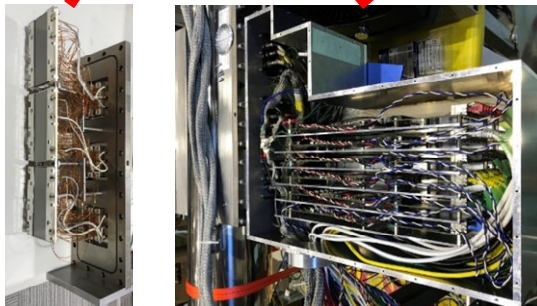
Former system	
Pulse width	125 ns
Sampling	250 μ s*

*Typically

Upgraded system	
Pulse width	5 ns
Sampling	10 μ s



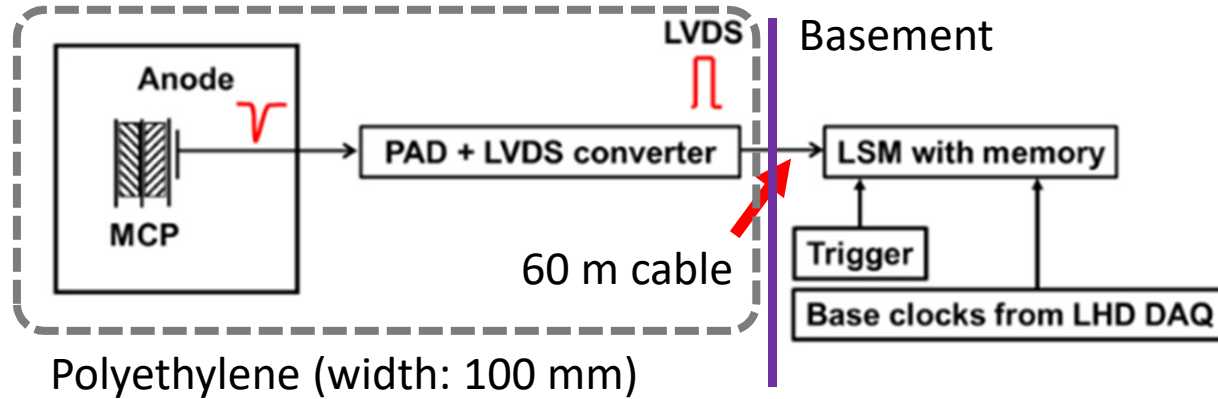
Signal of the test particle using Am a source



PAD: Preamplifier And Discriminator
LSM: Latching Scaler Module
EMM: External Memory Module

Neutron effect on E//B-NPA

We also upgrade in order to reduce the effect of neutrons to the E//B-NPA.

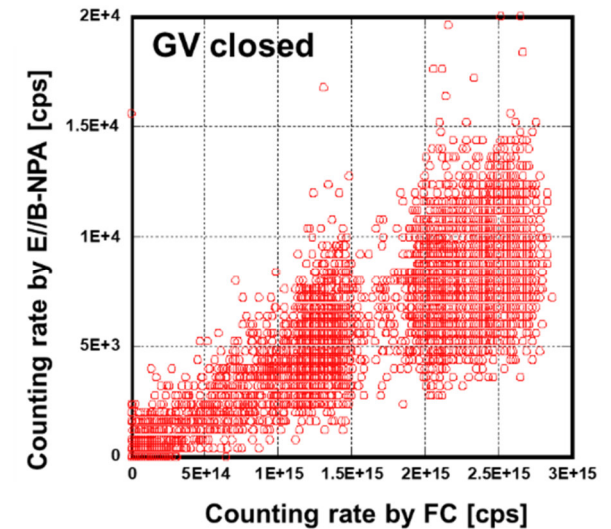
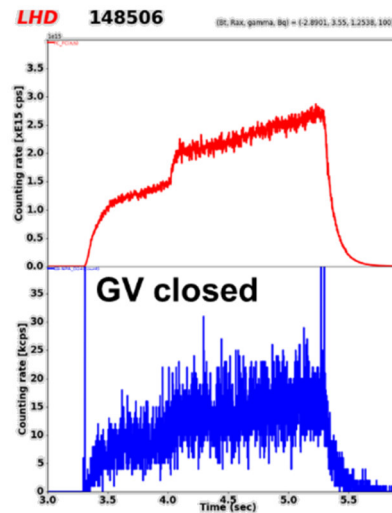


- ✓ Enclosed by 100 mm polyethylene blocks and 5 mm boron sheets.
- ✓ Moved the digitizer and controllers to the basement.

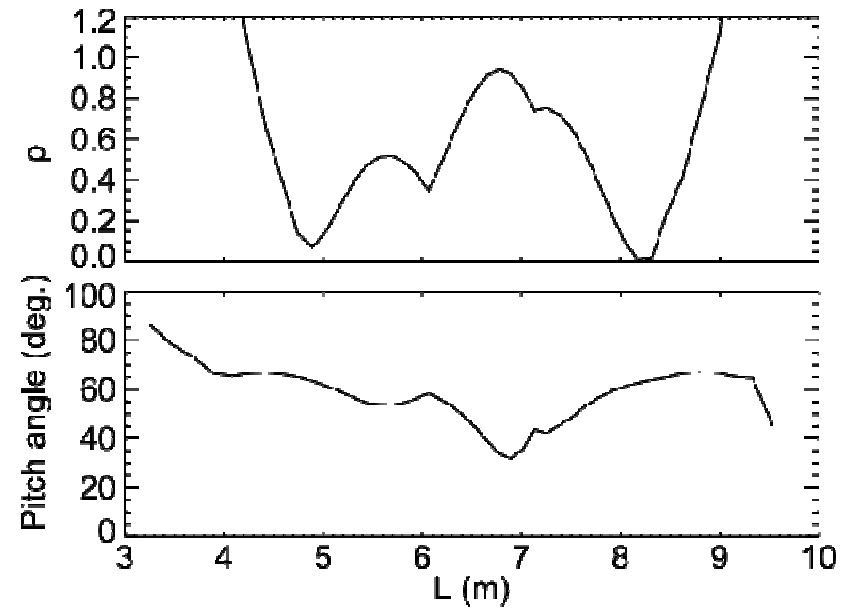
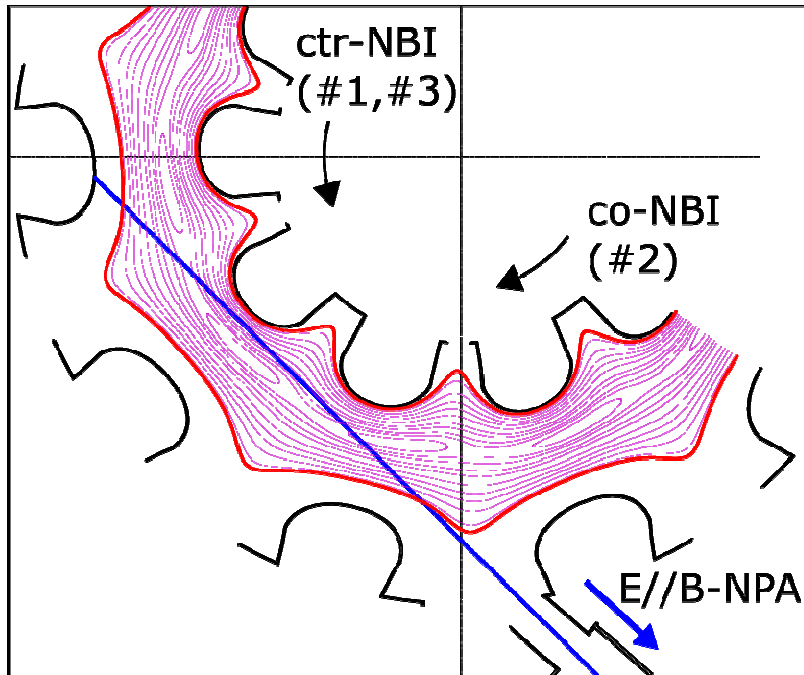


Power supply, vacuum gauge controller, etc.

The neutron effect was measured during the DD experiments with the gate valve closed.



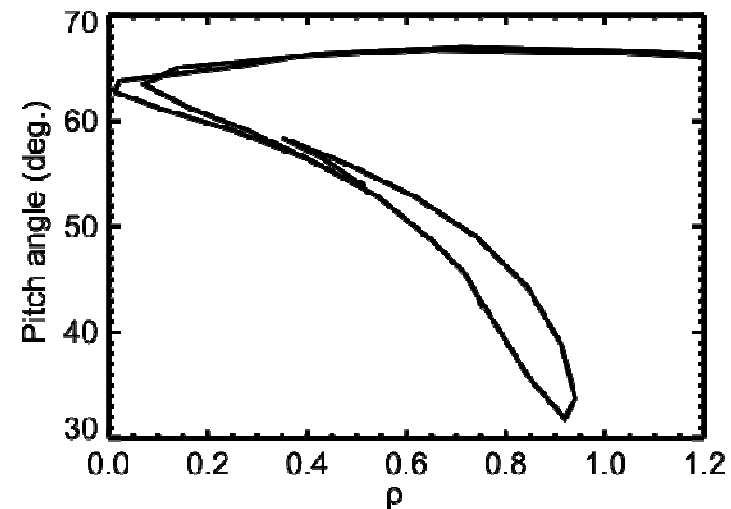
E//B-NPA line of sight



L is the length from the port.

The port to the stripping cell is 4.3 m.

- E//B-NPA can measure the energetic particles injected by NBI-#1 or #3.
- The neutral distribution is important because NPA measures the charge exchanged particles.
- The neutral density is very high at around $\rho=1$, and outside.

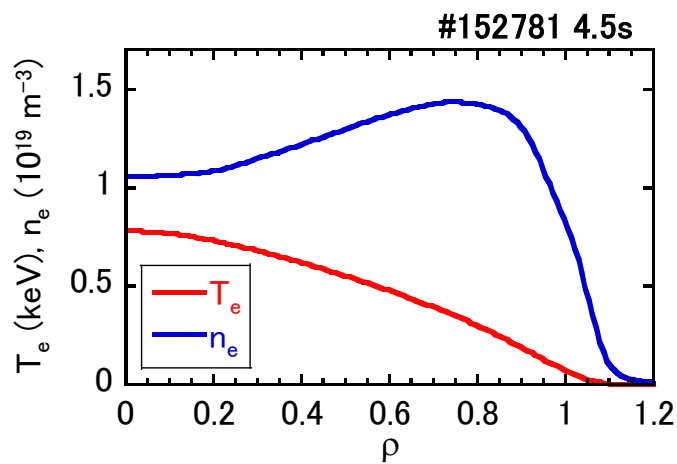


Experimental conditions of the TAE bursts

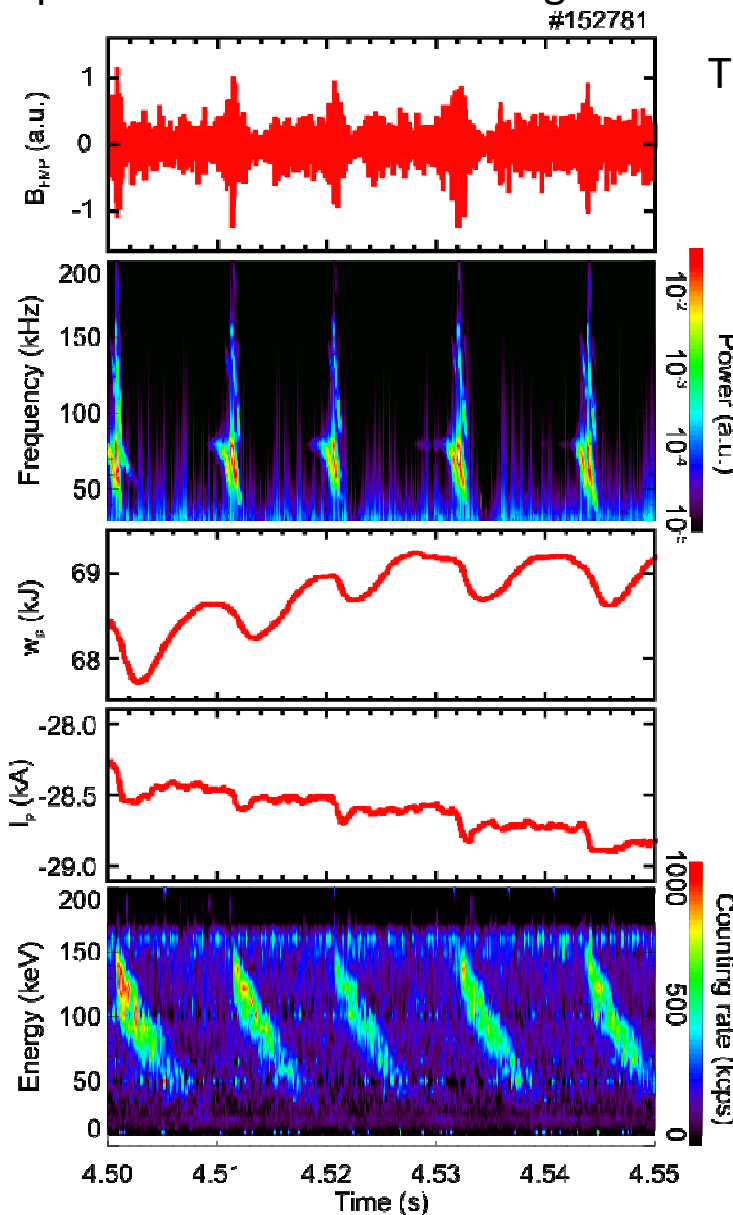
The TAE bursts are observed in experiment with the low magnetic field.

R_{ax}	3.8 m
B_{ax}	0.6 T
P_{NBI}	3.6 MW
E_{NBI}	180 keV
n_e	$1.3 \times 10^{19} \text{ m}^{-3}$
T_e	0.8 keV

Parameters during the TAE bursts



T_e and n_e measured by Thomson scattering



Time evolutions of the
Magnetic probe

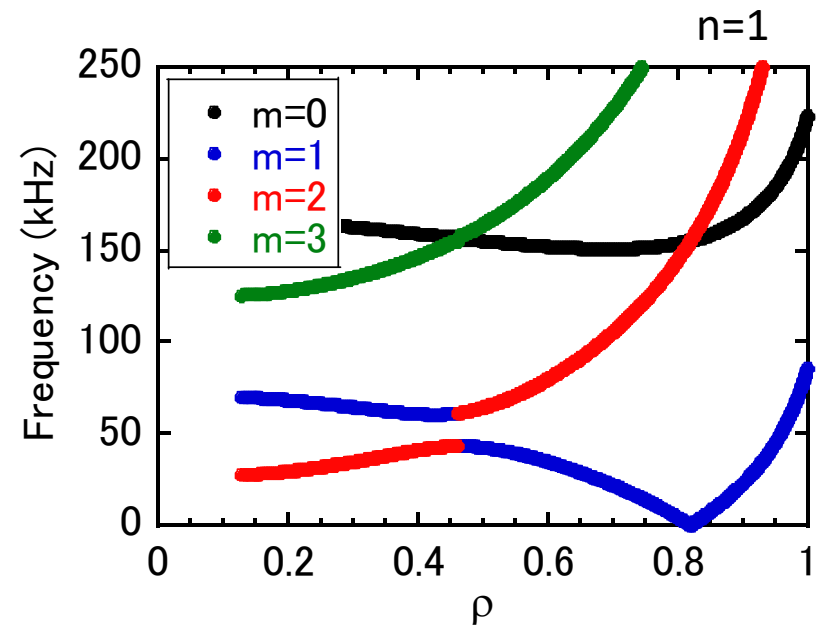
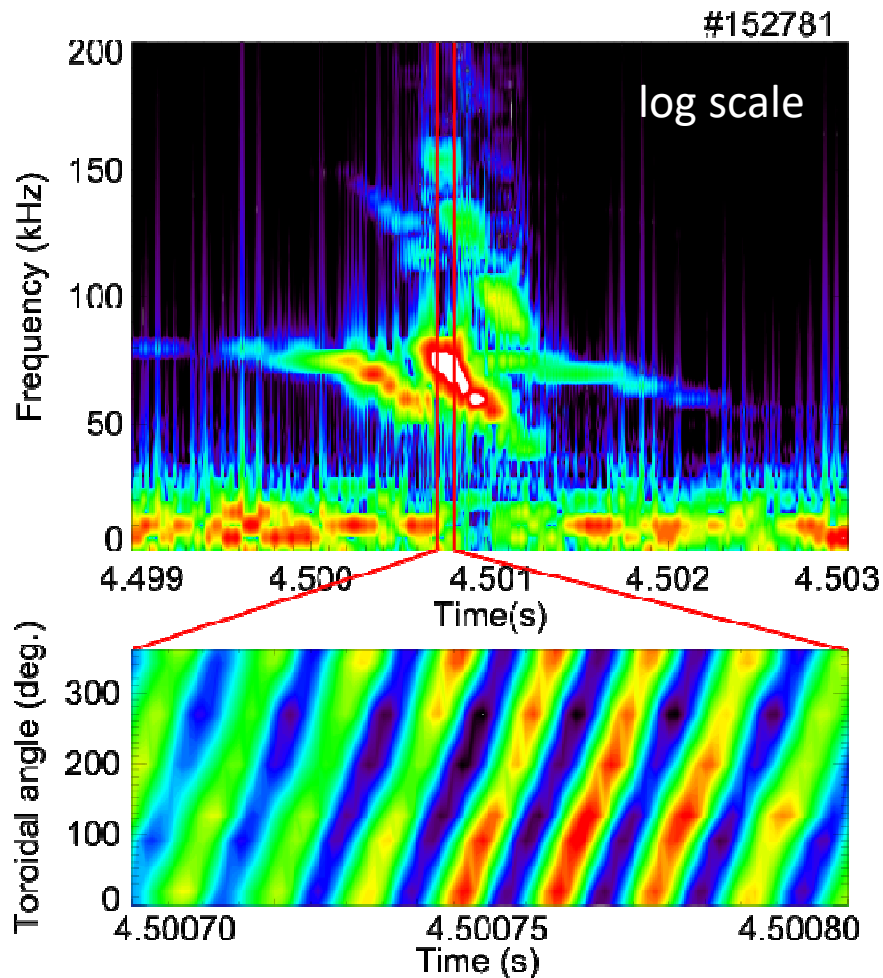
Magnetic probe
power spectrum

Stored energy

Plasma current

E//B-NPA

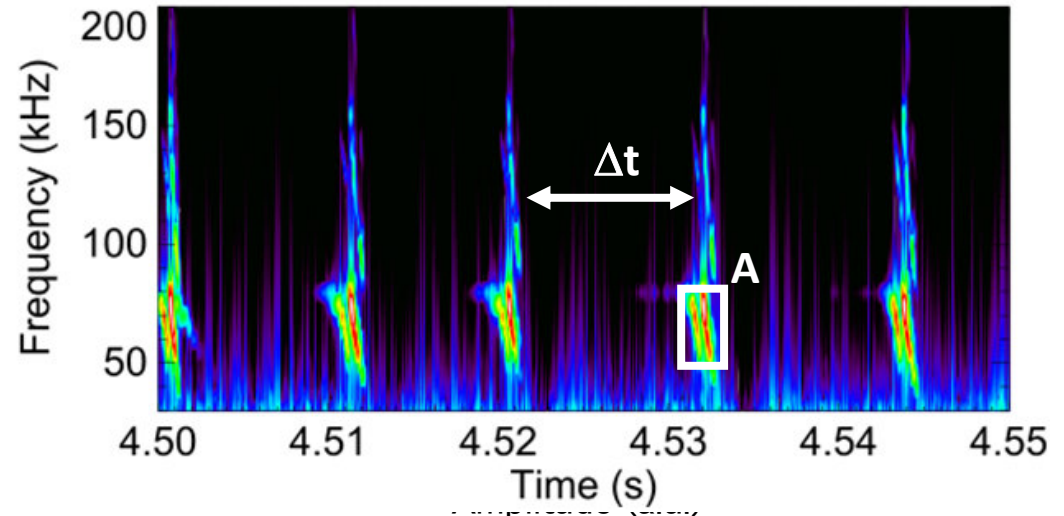
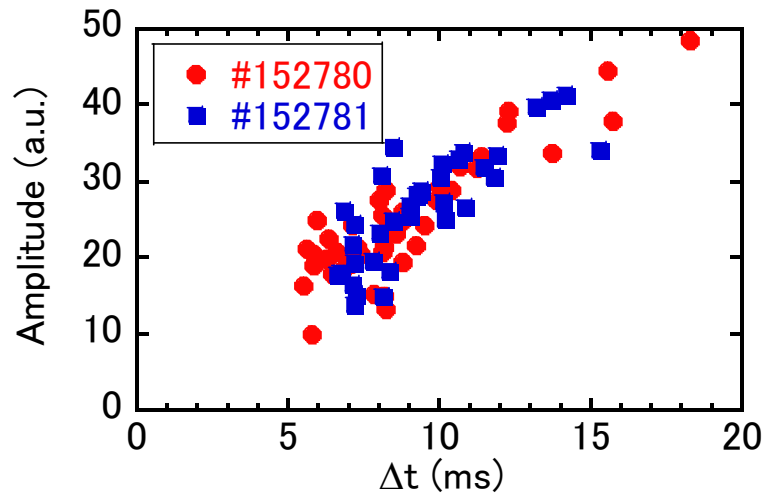
Toroidal and Poloidal mode analysis



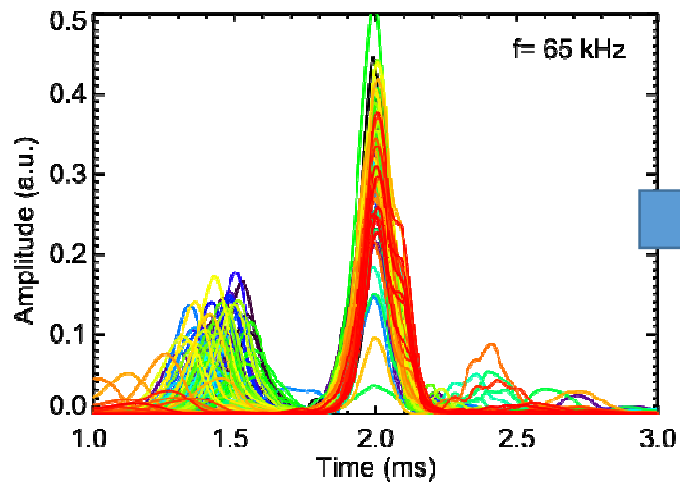
According to the calculated shear Alfvén spectrum, the location of the mode coupling is considered to be around $\rho=0.4-0.5$, with $m=1$ and $m=2$.

The toroidal mode number n is 1.

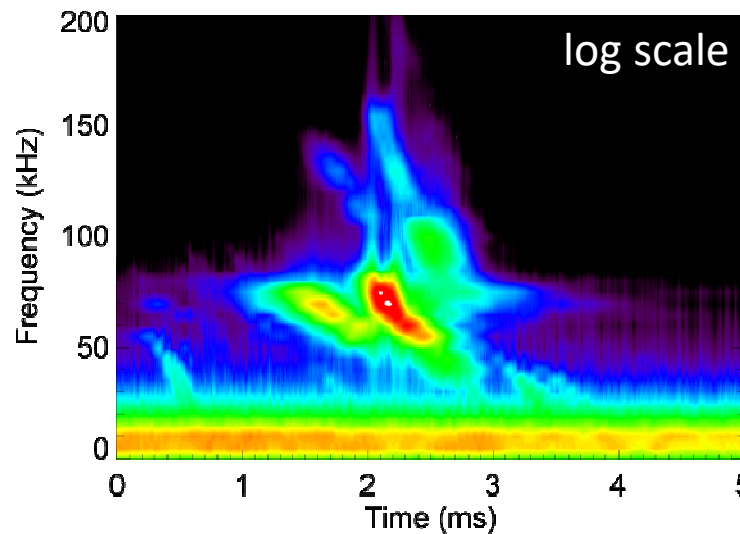
Investigation of the magnetic probes



Conditional averaging with the peak of the amplitude of $f=65\text{kHz}$

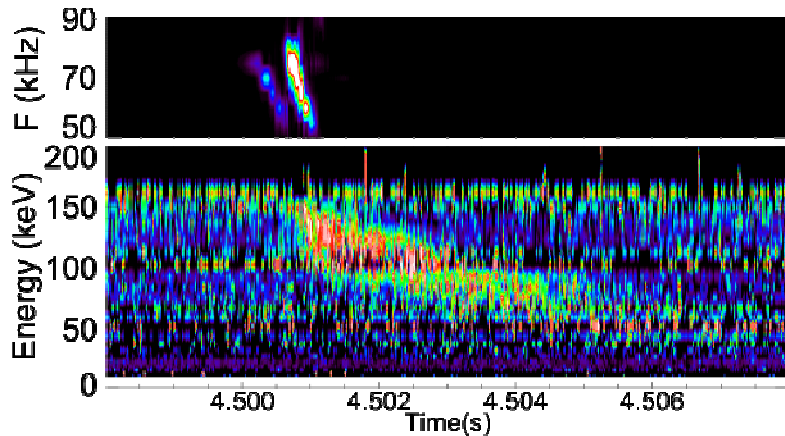


The amplitude of the Fourier power spectrum



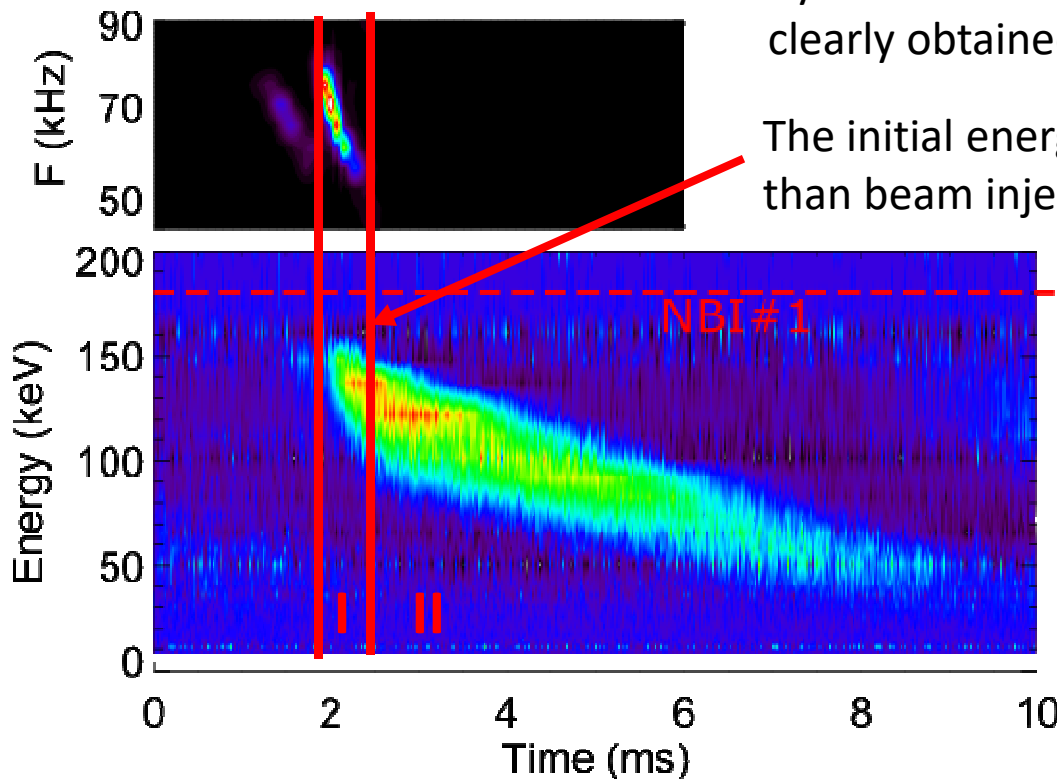
Small fluctuation is observed 0.3-0.5 ms before the large magnetic fluctuation.

Conditional averaging of E//B-NPA $\Delta\Gamma$



The energetic particles successfully observed with high time resolution. However, the count is not enough for the detailed discussion.

By the conditional average, the shape of the clump clearly obtained during and after the TAE bursts.



The initial energy is 150 keV, which is less than beam injection energy of 180 keV.

Phase I (during the TAE burst)

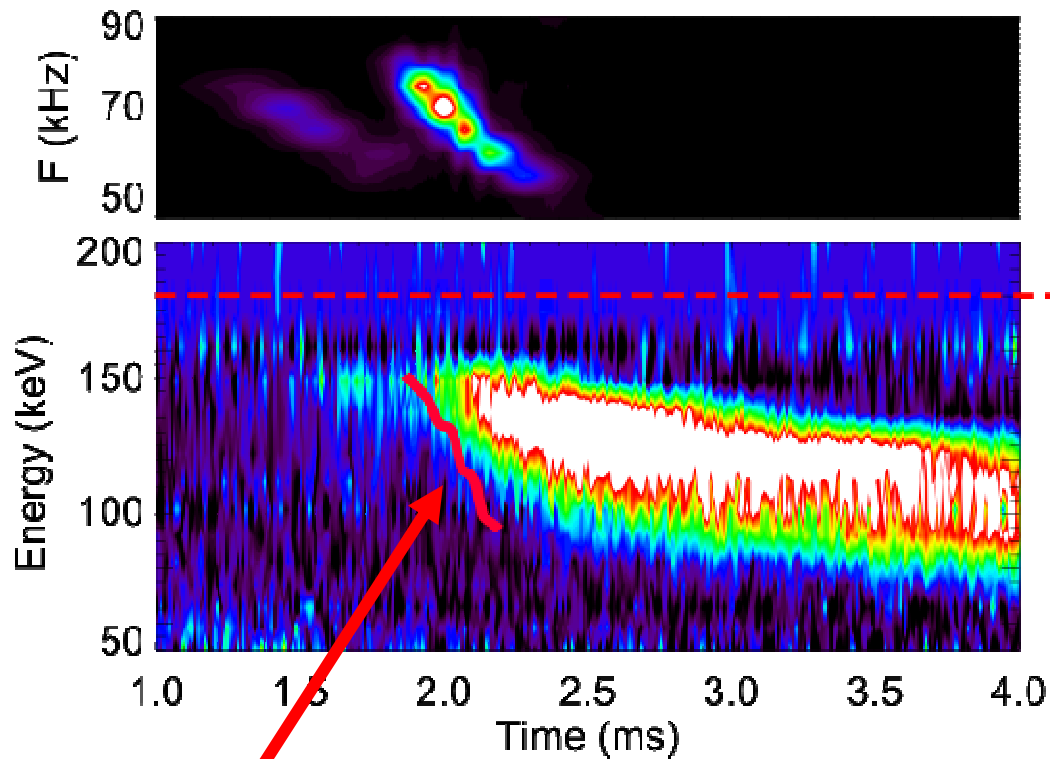
Observed particle flux increase and energy decrease. The frequency of the fluctuation also decrease.

Phase II (after the TAE burst)

Energy slowing down.

$\tau_s \sim 5.5-6.0$ ms

The energy of $\Delta\Gamma$ and v_A



$\Delta\Gamma$ increased after the peak of the magnetic fluctuation. The delay is approximately 0.1-0.3 ms.

The energy of the red line corresponds to the frequency of the TAE burst. The line is peak position of each frequency with the amplitude of at more than 0.15.

$$v_{\parallel} = v_A$$

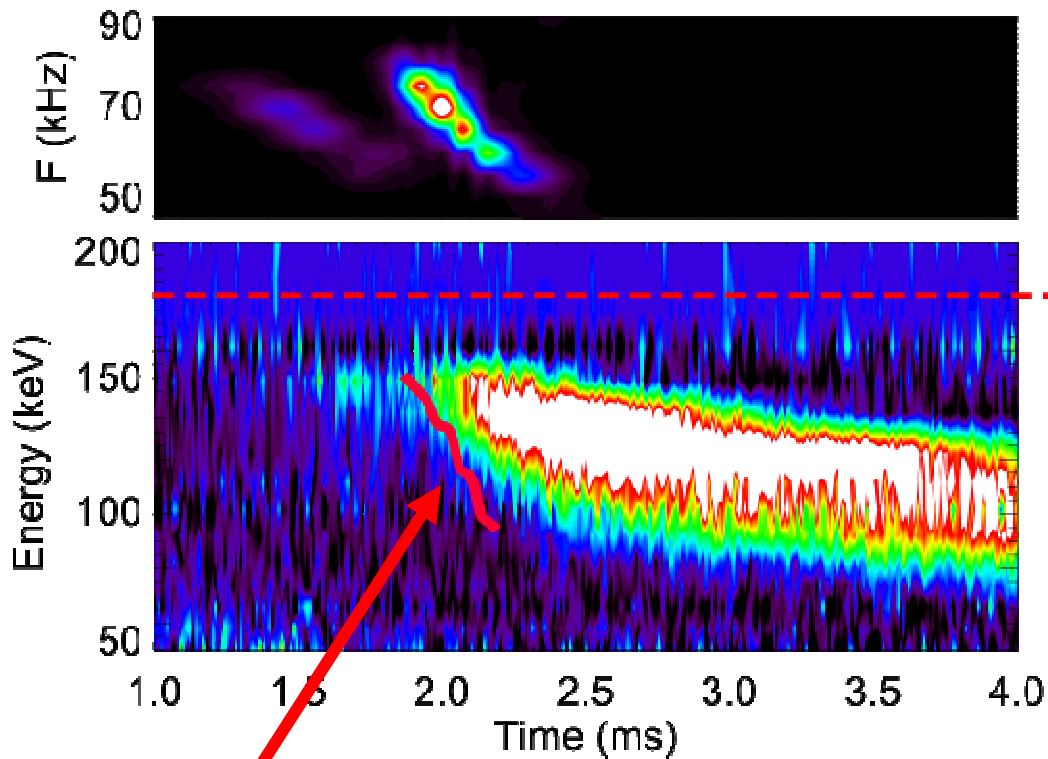
$$f_{\text{TAE}} = \frac{v_A}{4\pi q_{\text{TAE}} R}$$

$$v_A = (4\pi q_{\text{TAE}} R) f_{\text{TAE}}$$

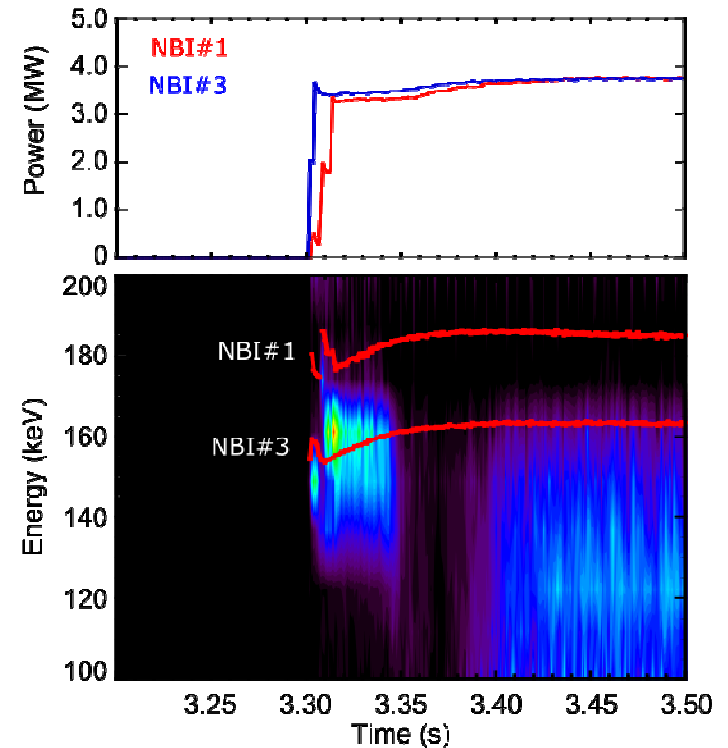
$$q_{\text{TAE}} = \frac{m + 1/2}{n}$$

The observed TAE frequency can be overplotted to the particle energy which is interacting with the TAE. v_A is similar to the observed particle energy by $E//B$ -NPA.

The energy of $\Delta\Gamma$ and v_A



$\Delta\Gamma$ increased after the peak of the magnetic fluctuation. The delay is approximately 0.1-0.3 ms.



Just in case, we checked the timing of the E//B-NPA. At the plasma start up, the injected beam was detected at the same time.

$$v_{\parallel} = v_A$$

$$f_{\text{TAE}} = \frac{v_A}{4\pi q_{\text{TAE}} R}$$

$$v_A = (4\pi q_{\text{TAE}} R) f_{\text{TAE}}$$

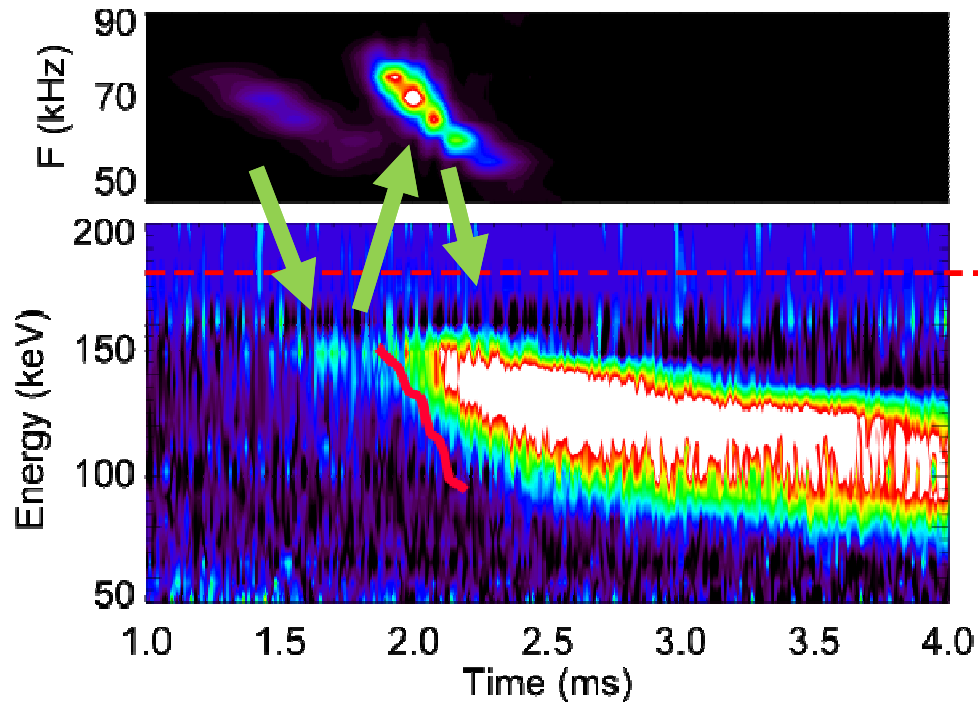
$$q_{\text{TAE}} = \frac{m + 1/2}{n}$$

The observed TAE frequency can be overplotted to the particle energy which is interacting with the TAE. v_A is similar to the observed particle energy by E//B-NPA.

E//B-NPA $\Delta\Gamma$ with Alfvén velocity

Small fluctuation \rightarrow 150 keV particles observed

\rightarrow Large fluctuation \rightarrow Much higher counting rate and slowing down

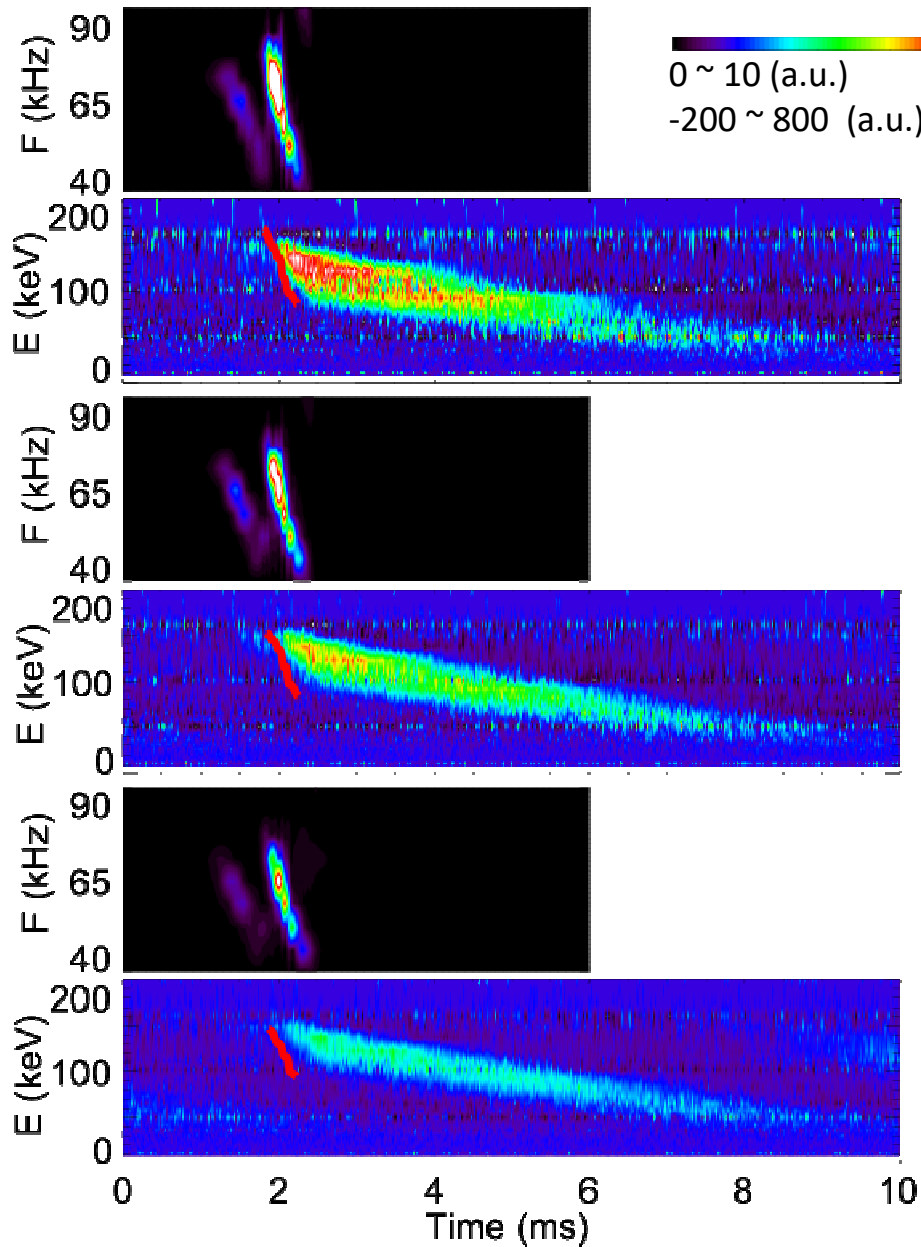


- ◆ 140-150 keV particles are observed before the large magnetic fluctuation.
- ◆ The causal relationships between the pre-burst, initial $\Delta\Gamma$ and burst are not clear. Follow-up experiments and simulations are future works.
- ◆ The velocity of the initial $\Delta\Gamma$ of 150 keV corresponds to $f=77$ kHz. Therefore, the initial $\Delta\Gamma$ is considered to be the interacted with TAE.

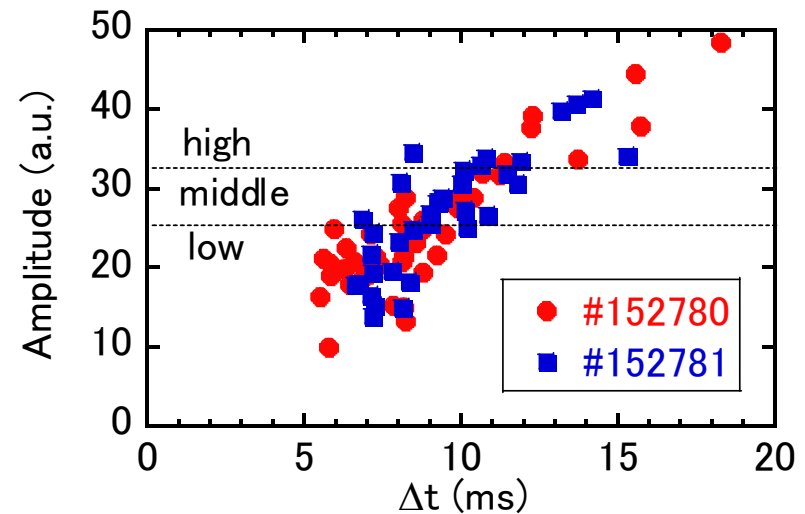
The upgraded high time resolution E//B-NPA enable us to measure the details during the TAE bursts.

Fine time steps also allow more accurate conditional averaging.

Conditional averaging of E//B-NPA $\Delta\Gamma$

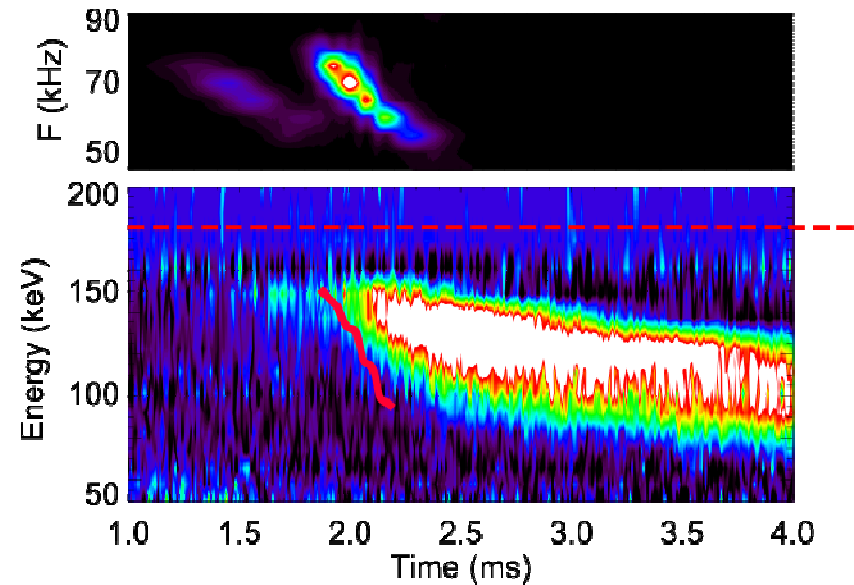
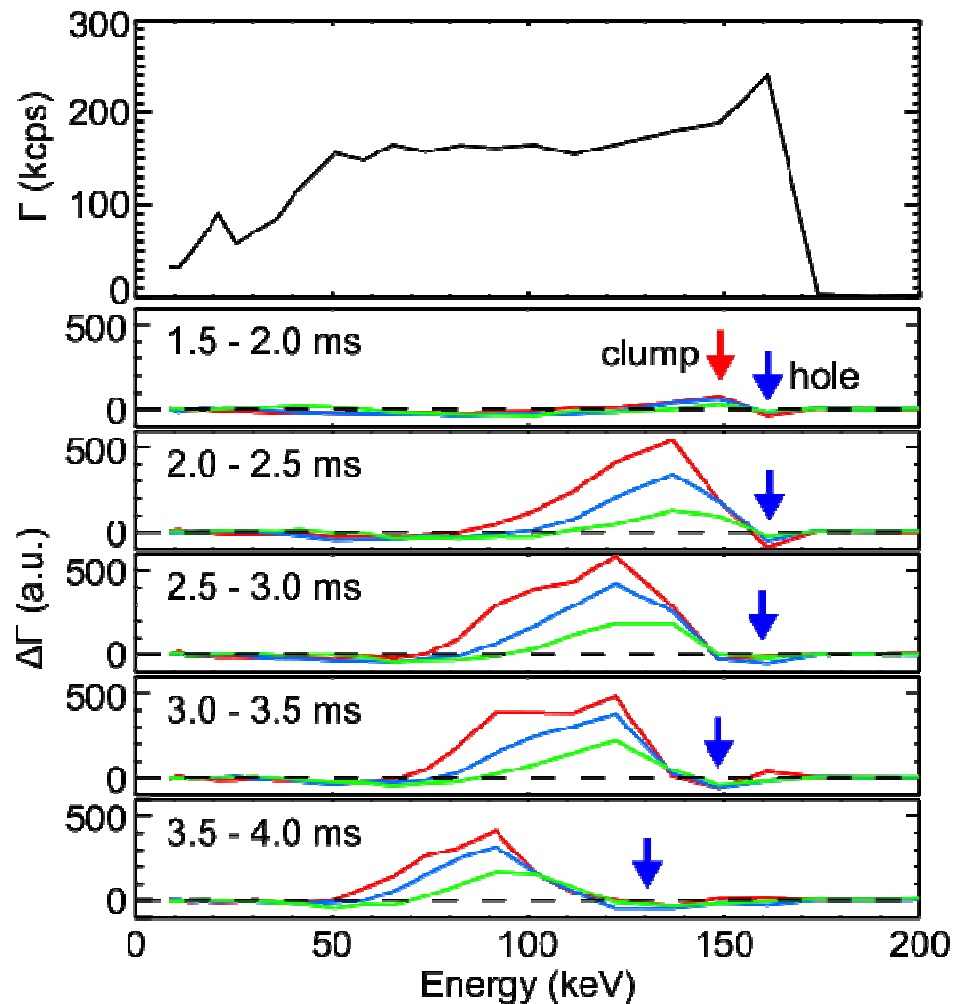


Here, we divided into three groups by the amplitudes of the TAE fluctuations, and conditional averaged.



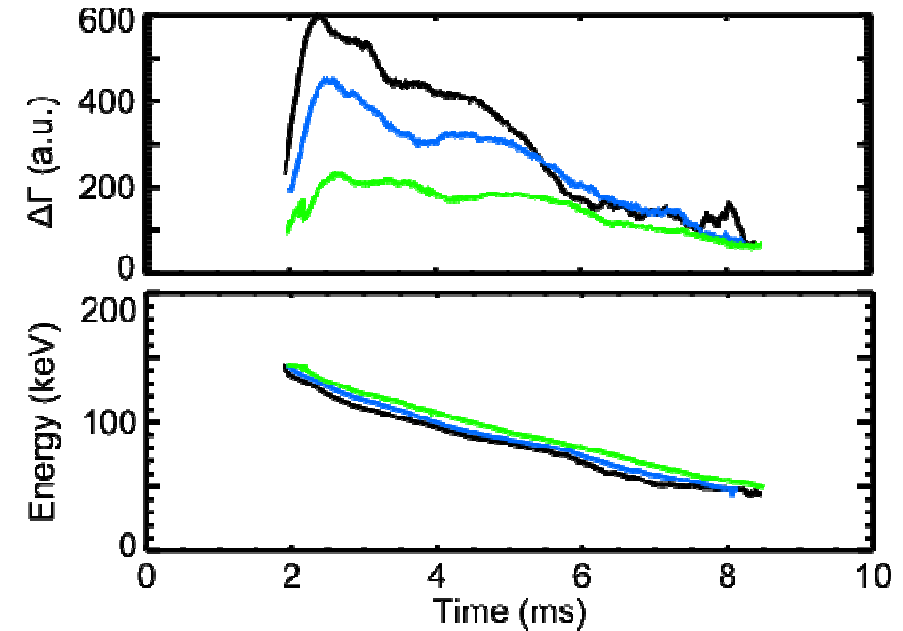
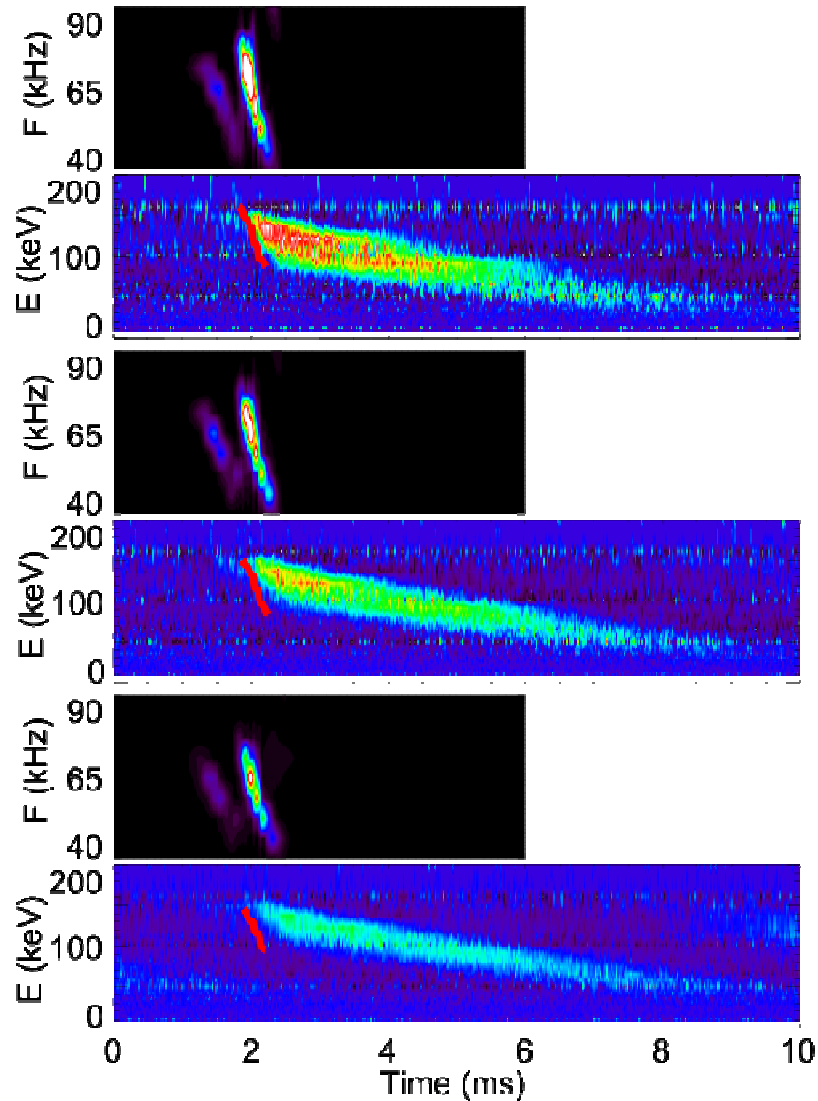
The energy spectrum of the observed clump is wider at the higher amplitude of the TAE bursts case. The energy range of the magnetic fluctuations are also wide.

The observed hole of E//B-NPA $\Delta\Gamma$



Because we observed higher $\Delta\Gamma$ than Γ , hole is difficult to be recognized clearly. However, the hole is also observed at the higher energy range than the clump observed.

Slowing down after the TAE bursts



Decreased $\Delta\Gamma$ indicates the orbit shift to the out of line of sight. We can only measure the particles which charge exchanged at along the line of sight. Therefore, if the clump scattered, $\Delta\Gamma$ should be decreased.

Decreasing of the energy indicates the energy slowing down. The slowing down time is 5.5-6.0 ms.

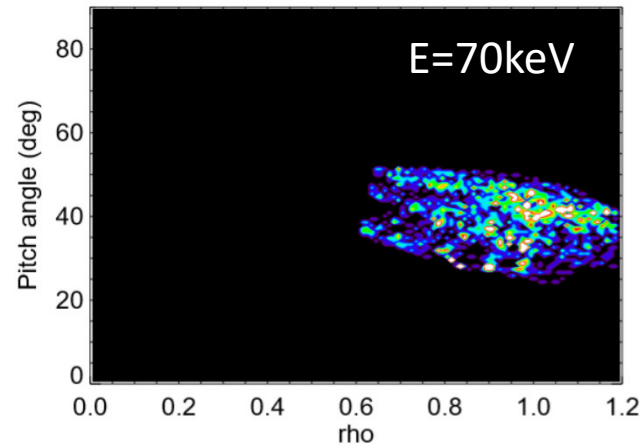
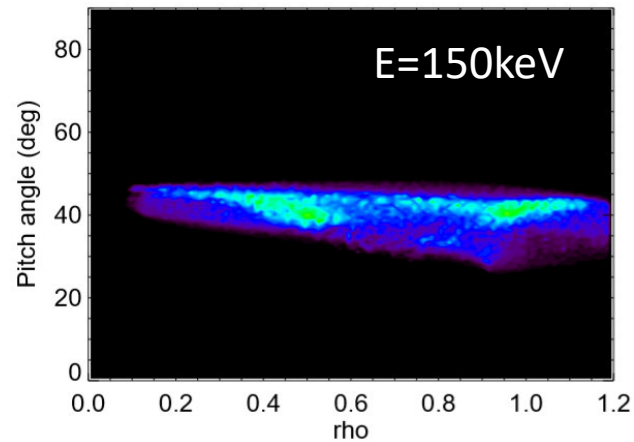
Summary

- ❑ In order to investigate the TAE bursts in more detail, the E//B-NPA was upgraded.
- ❑ The time resolution was improved up to 100 kilo sampling per second.
- ❑ During the TAE bursts, the clump and the hole were observed in the similar energy with the phase velocity of $v_{//} = v_A$.
- ❑ The time delay of the clump detection from the peak amplitude of the magnetic fluctuation is 0.1-0.3 ms.

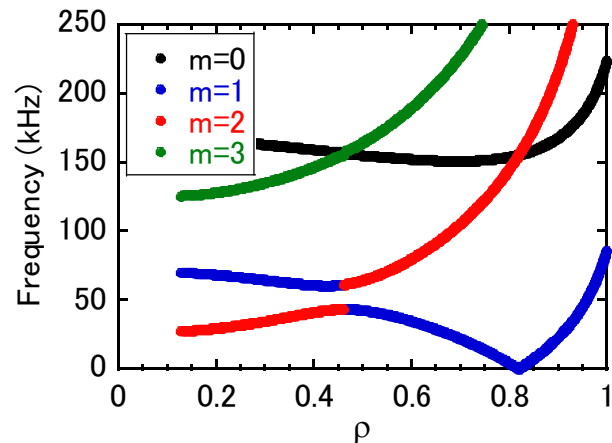
Slowing down after the TAE burst

Test results of the orbit trace code lorbit

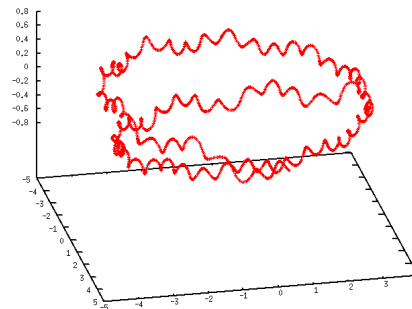
$R=4.2705$ m ($\rho \sim 1$)



Color: 0-2 μs



$R=4.2705$ m, $T = 14 \mu\text{s}$



Toroidal Alfvén Eigenmode (TAE)

$$v_A = \sqrt{\frac{B^2}{\mu_0 \rho_{m0}}}$$

$$\omega^2 = k_{\parallel}^2 v_A^2$$

$$k_{\parallel} = \frac{\mathbf{k} \cdot \mathbf{B}}{B} = \frac{1}{R} \frac{n - m}{q}$$

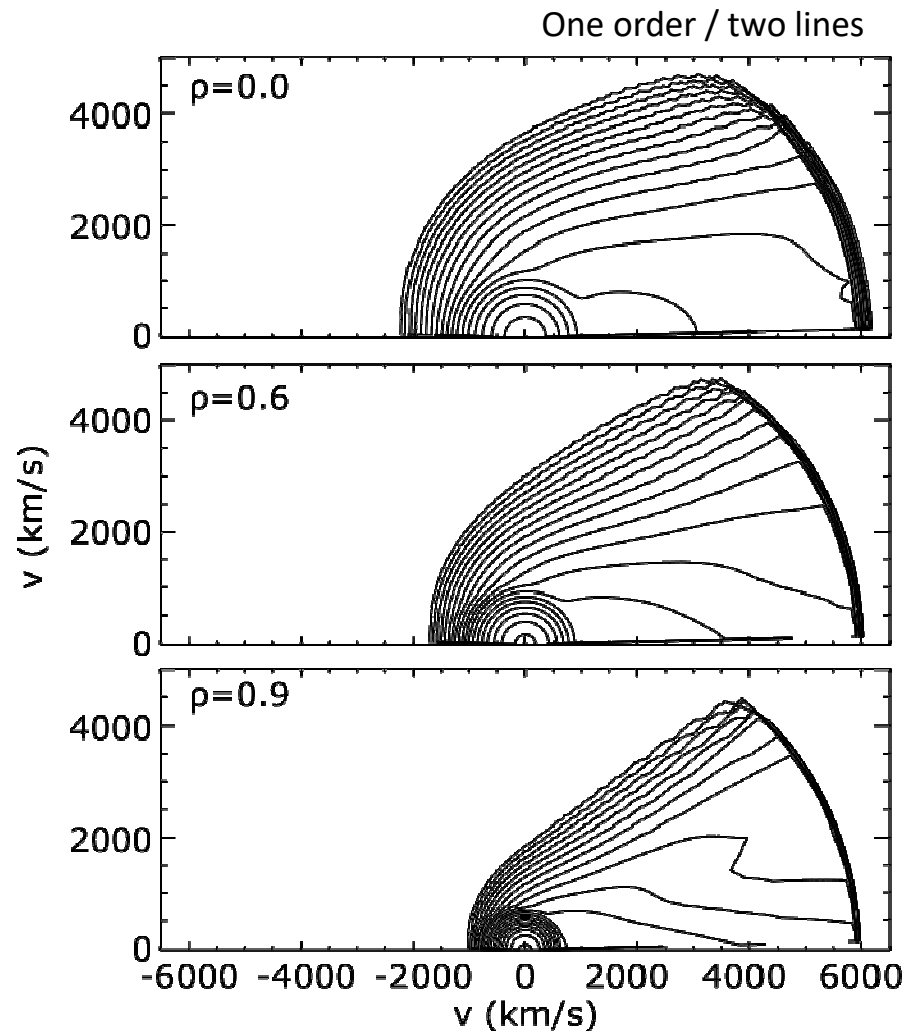
$$k_{\parallel m} = -k_{\parallel m+1}$$

$$q_{\text{TAE}} = \frac{m + 1/2}{n}$$

$$f_{\text{TAE}} = \frac{v_A}{4\pi q_{\text{TAE}} R}$$

Simulation by TASK/FP

Energy distributions of the energetic particles calculated by Fokker Planck simulation



TASK/FP is a Fokker-Planck code to calculate the time evolution of momentum function f in three dimension: (p, θ, ρ)

$$\frac{\partial f_s}{\partial t} = -\nabla_p \cdot S + H$$

$$H = S_{\text{NB}} + L_{\text{CX}}(f) + S_{nf}(f) + L_{\text{sink}}(f) + R(f)$$

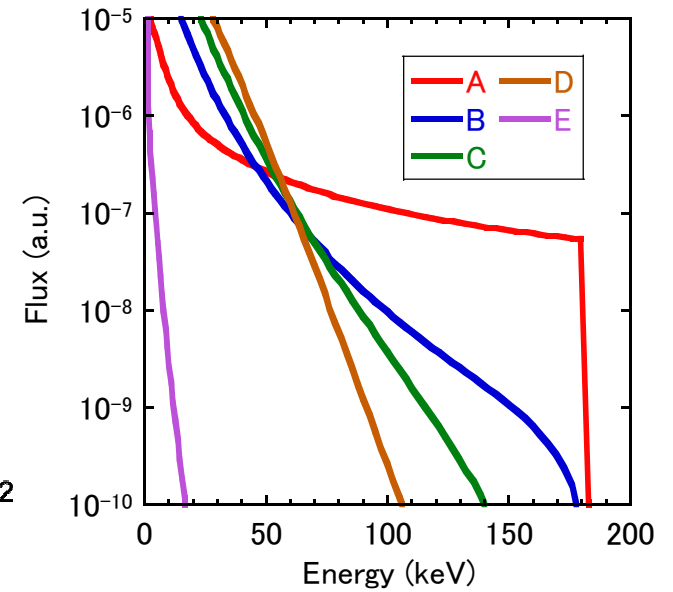
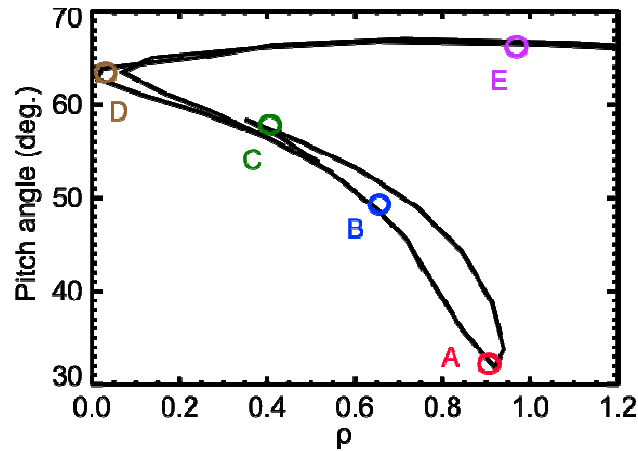
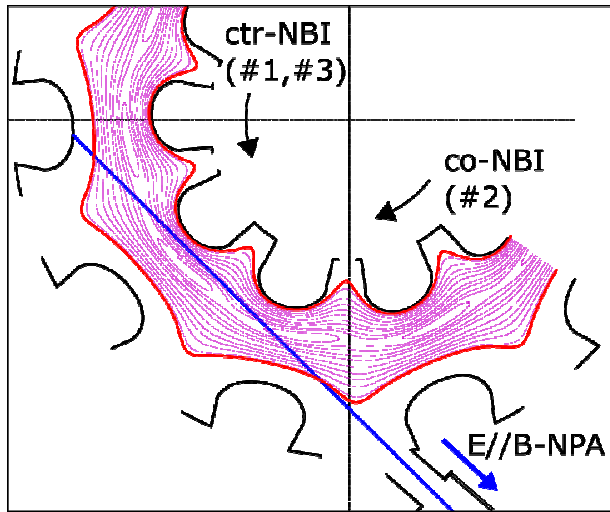
H includes beam source, charge exchange loss, fusion reaction source and loss, artificial loss, and radial diffusion terms.

In present, the radial diffusion term is not used.

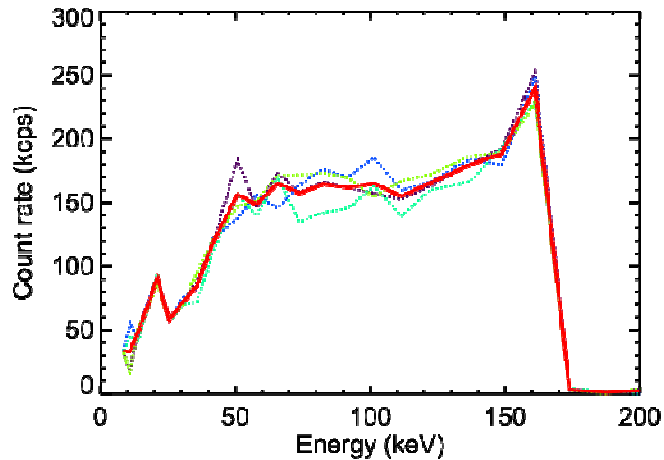
H. Nuga *et al.*, *Nucl. Fusion* **57** (2017) 086011

H. Nuga *et al.*, *Nucl. Fusion* **59** (2019) 016007

Simulation by TASK/FP



The particles which observed by E//B-NPA considered to charge exchange at around the point **A**.



At the point **A**, v_A is 5.2×10^6 m/s